Available online at www.sciencedirect.com
ScienceDirect
Journal of Power Sources 163 (2007) 892–899
JOURNAL OF POWER SOURCES
www.elsevier.com/locate/jpowsour

Influence of current densities in SOFC and PEFC stacks on a SOFC–PEFC combined system

M. Yokoo [a,*], K. Watanabe [a], M. Arakawa [a], Y. Yamazaki [b]

[a] *NTT Energy and Environment Systems Laboratories, NTT Corporation, 3-1, Morinosato-Wakamiya, Atsugi-shi, Kanagawa 243-0198, Japan*

[b] *Department of Innovative and Engineered Materials, Interdisciplinary Graduate School of Science and Engineering, Tokyo Institute of Technology, 4259, Nagatsuta, Midoriku, Yokohama-shi, Kanagawa 226-8502, Japan*

Received 7 August 2006; received in revised form 25 September 2006; accepted 27 September 2006
Available online 13 November 2006

Abstract

A solid oxide fuel cell (SOFC)–polymer electrolyte fuel cell (PEFC) combined system was investigated by numerical simulation. Here, the effect of the current densities in the SOFC and the PEFC stacks on the system's performance is evaluated under a constant fuel utilization condition. It is shown that the SOFC–PEFC system has an optimal combination of current densities, for which the electrical efficiency is highest. The optimal combination exists because the cell voltage in one stack increases and that of the other stack decreases when the current densities are changed. It is clarified that there is an optimal size of the PEFC stack in the parallel-fuel-feeding-type SOFC–PEFC system from the viewpoint of efficiency, although a larger PEFC stack always leads to higher electrical efficiency in the series-fuel-feeding-type SOFC–PEFC system. The 40 kW-class PEFC stack is suitable for the 110 kW-class SOFC stack in the parallel-fuel-feeding type SOFC–PEFC system.
© 2006 Elsevier B.V. All rights reserved.

Keywords: Solid oxide fuel cell; Polymer electrolyte fuel cell; Combined system; Steam reforming

1. Introduction

Power-generating systems using a solid oxide fuel cell (SOFC) stack provide high electrical efficiency because the high-temperature SOFC exhaust heat (≈1073 K) can be used for fuel reforming and because activation and ohmic losses are low due to the high operation temperature [1]. A system using an SOFC stack only (simple SOFC system) has achieved a 46% electrical efficiency at 109 kW ac [2]. However, power-generation systems in which an SOFC stack is used in combination with other generating equipment can provide higher electrical efficiency than the simple SOFC system [1]. This is because the high-temperature SOFC exhaust heat also contributes to power generation in the other generating equipment.

Although systems combining an SOFC stack and a gas turbine (SOFC–GT systems) have been widely studied [3–6], systems combining an SOFC stack with a polymer electrolyte fuel cell (PEFC) stack are attracting attention [7–11]. High-temperature SOFC exhaust heat is used to produce hydrogen for a PEFC stack in SOFC–PEFC systems. The high-temperature SOFC exhaust heat is a promising heat source in a combined power and hydrogen station [7]. The features of the SOFC–PEFC system are as follows: the SOFC–PEFC system is quieter than SOFC–GT system and the cost of the auxiliary equipment is lower [9]. In addition, SOFC–PEFC systems can provide a higher efficiency than SOFC–GT systems when the output is relatively small. This follows from the fact that the efficiency of the PEFC stack remains almost constant even as the scale of the stack decreases, whereas that of the GT efficiency decreases as the scale decreases [9–11].

The SOFC–PEFC systems can be classified into two types depending on the fuel-feeding method [11]. One is an SOFC–PEFC system in which all fuel is fed to the SOFC stack first and then SOFC exhaust fuel is fed to the PEFC stack. This type of SOFC–PEFC system is called a series SOFC–PEFC system in this paper. The other is an SOFC–PEFC system in which a part of reformed fuel is fed to the SOFC stack and the remaining

* Corresponding author. Tel.: +81 46 240 2572; fax: +81 46 270 2702.
E-mail address: m.yokoo@aecl.ntt.co.jp (M. Yokoo).

0378-7753/$ – see front matter © 2006 Elsevier B.V. All rights reserved.
doi:10.1016/j.jpowsour.2006.09.050

Nomenclature

C	constant
E	electromotive force (V)
F	Faraday's constant (C mol^{-1})
I	total current in stack (A)
J	current density (A m^{-2})
M	molar flow rate (mol s^{-1})
Q	amount of heat (W)
S	total electrode area (m^2)
U	utilization (%)
V	cell voltage (V)
W	output (W)

Greek letters

α	parameter for determining the PEFC stack performance
η	electrical efficiency (%)

Subscripts

ac	alternate current
AIR	air
ANO	anode
FUEL	fuel
Max	maximum
PE	PEFC
Rated	rated
REF	reform
SIMP	simple SOFC system
SO	SOFC
SYS	system

fuel is fed to the PEFC stack. This type of SOFC–PEFC system is referred to as a parallel SOFC–PEFC system in this paper. These SOFC–PEFC systems were evaluated quantitatively under the constant current density condition, in which the current densities of the both stacks are kept constant, in our previous paper [11] and it was found that the electrical efficiency increases with the power output of the PEFC stack.

In a simple SOFC or PEFC system, the lower current density in the stack always leads to higher electrical efficiency when the fuel utilization is kept constant, because the cell voltage is higher when the average current density is lower. However, it is not clear how the system performance is changed when the current densities in both stacks are varied under the constant fuel utilization condition, in which the total fuel utilization in the combined system is kept constant. This is because the cell voltage in one stack increases and that in the other decreases when the current densities are varied. In this paper, the effect of the current densities in both stacks is evaluated quantitatively under the constant fuel utilization condition on the basis of numerical simulation. This evaluation clarifies the investigation of influence of fuel utilization in each stack in the combined system.

2. System models and exhaust heat utilization mechanism

The system models and the exhaust heat utilization mechanism are the same as those used in our previous studies [9,11]. Therefore, they are only briefly explained here.

Schematic diagrams of the parallel and series SOFC–PEFC systems are shown in Figs. 1 and 2, respectively. A sealless tubular SOFC stack with a depleted fuel recycling plenum and steam reformer is used for the model of the SOFC stack. In the parallel SOFC–PEFC system, part of the reformed fuel is fed to the tubular SOFC and the rest is fed to the PEFC stack. In contrast, in the series SOFC–PEFC system, all reformed fuel is fed to the tubular SOFC first and part of the SOFC anode exhaust gas is fed to the PEFC stack. The carbon monoxide in the reformed gas or the SOFC anode exhaust gas fed to the PEFC stack is removed as they pass through the shift converter and CO selective oxidizer. Part of the SOFC exhaust gas is recycled to the reformer to feed steam. The recycle gas flow rate is chosen so that the steam-to-methane molar fraction (S/C ratio) at the reformer inlet is 3.0. In this paper, it is assumed that the system cannot be constructed when the S/C ratio is not kept at 3.0, although it is possible to construct it by supplying external steam. This is because a large amount of energy has to be used to evaporate the external steam and raise its temperature in these SOFC–PEFC systems. Such energy loss can lead to reduced electrical efficiency.

The SOFC exhaust heat utilization mechanism used in the simulation is illustrated in Fig. 3, where Q_{REF} is the SOFC exhaust heat used in the steam reformer as reaction heat and Q_{AIR} is the SOFC exhaust heat discharged with air for the SOFC.

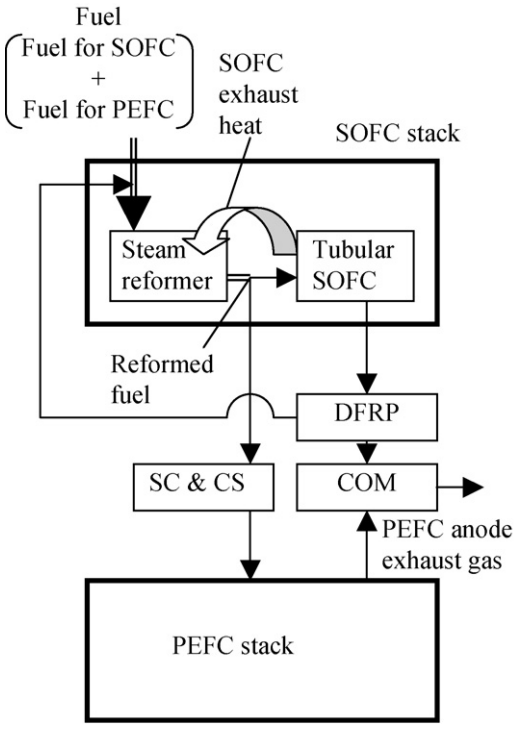

Fig. 1. Parallel SOFC–PEFC system. COM, combustor; CS, CO selective oxidizer; DFRP, depleted fuel recycling plenum; SC, shift converter.

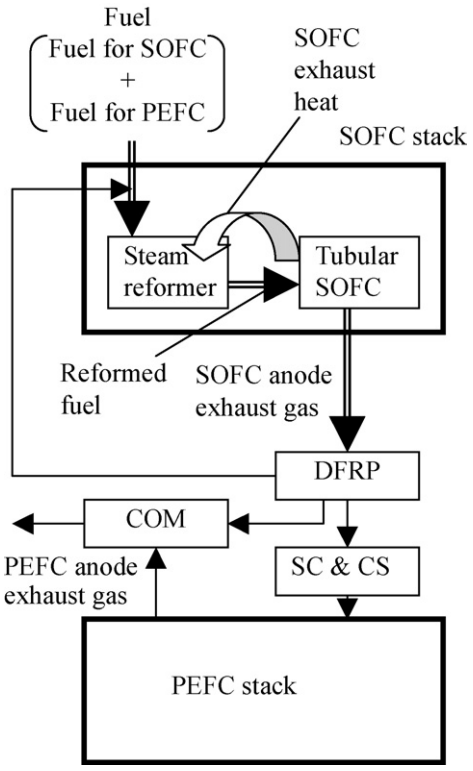

Fig. 2. Series SOFC–PEFC system. COM, combustor; CS, CO selective oxidizer; DFRP, depleted fuel recycling plenum; SC, shift converter.

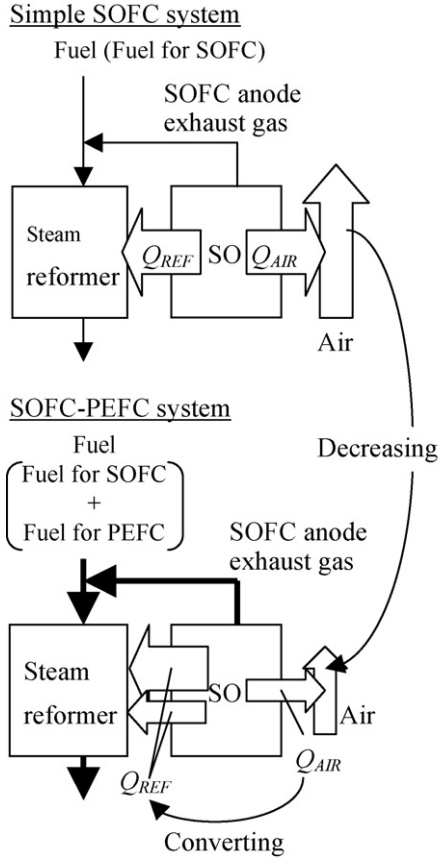

Fig. 3. SOFC exhaust heat utilization mechanism.

The Q_{REF} can be increased by converting the decrement of Q_{AIR} to Q_{REF} while the SOFC operation temperature is kept constant.

3. Simulation

The simulation was performed to quantitatively evaluate the influence of the current densities in SOFC and PEFC stacks under the constant fuel utilization condition. The electrode area of the SOFC stack was assumed to be the same for both kinds of SOFC–PEFC systems. As the simulation parameter, the electrode area of the PEFC stacks in the SOFC–PEFC systems was varied.

3.1. Sealless tubular SOFC stacks

The electrode area of the tubular SOFC is the same as that of the tubular SOFC in an actual simple 110 kW-class SOFC system [2], which means that the SOFC stack is 110 kW class. The steam reformer is installed adjacent to the tubular SOFC. The temperature profiles of the electrolyte and the cell voltage in the SOFC stack V_{SO} are calculated the same way as in our previous studies [9,11]. The total current in the SOFC stack I_{SO} is

$$I_{SO} = S_{SO} J_{SO}, \tag{1}$$

where S_{SO} is the total electrode area and J_{SO} is the current density in the SOFC stack.

In the parallel SOFC–PEFC system, the flow rate of the reformed fuel fed to the PEFC $M_{REF\text{-}PE}$ is

$$M_{REF-PE} = M_{REF} - M_{REF-SIMP}, \tag{2}$$

where M_{REF} is the flow rate of the reformed fuel and $M_{REF\text{-}SIMP}$ is that of the reformed fuel in the simple SOFC system. That is, the flow rate of reformed gas fed to the tubular SOFC is kept constant in the parallel SOFC–PEFC system. In the series SOFC–PEFC system, the flow rate of the SOFC anode exhaust gas fed to the PEFC stack $M_{SO\text{-}ANO\text{-}PE}$ is

$$M_{SO-ANO-PE} = M_{SO-ANO} - M_{SO-ANO-SIMP}, \tag{3}$$

where $M_{SO\text{-}ANO}$ is the flow rate of the SOFC anode exhaust gas and $M_{SO\text{-}ANO\text{-}SIMP}$ is that of the SOFC anode exhaust gas in the simple SOFC system.

3.2. PEFC stacks

The rated net ac output $W_{PE\text{-}Rated}$ is defined as the output when the cell voltage is 0.75 V and the current density is 2000 A m^{-2} [12]. The cell voltage of 0.75 V is referred to as the designed voltage for the PEFC in this paper. As a simulation parameter, the electrode area of the PEFC stacks was varied. In the parallel SOFC–PEFC systems, the total electrode area of the PEFC stacks was determined on the basis of actual PEFC stack performance [12] so that the rated net ac outputs of the PEFC stacks would be 10, 20, 30, 40, 50, 60 or 70 kW. In the series SOFC–PEFC systems, the total electrode area of the PEFC stacks was determined so that the rated net ac outputs of the

PEFC stacks would be 5, 10, 15, 20, 25, 30 or 35 kW. The operation temperature of the PEFC was assumed to be 343 K. The partial pressure of steam in the fuel and in the air fed to the PEFC stack is the saturation vapor pressure at 343 K. The electromotive force of the PEFC E_{PE} was assumed to be average of those at the PEFC inlet and outlet [11]. The voltage in the PEFC stack V_{PE} is calculated using

$$V_{PE} = E_{PE} - \alpha \left(C_1 J_{PE} + C_2 \ln \frac{J_{PE}}{C_3} \right). \quad (4)$$

Here, α is a comparative index and equal to 1.0 for the actual PEFC stack performance. Therefore, α is basically 1.0 unless mentioned otherwise. The value of 0.8 or 1.2 was used as the value for α to investigate the effect of the *I–V* characteristics of PEFC stack. The values for C_1, C_2 and C_3 are $2.12 \times 10^{-5}\ \Omega\,m^2$, 4.07×10^{-2} V and $1.35\ A\,m^{-2}$, respectively [11]. The total current in the PEFC stack I_{PE} is

$$I_{PE} = S_{PE} J_{PE}, \quad (5)$$

where S_{PE} is the total electrode area and J_{PE} is the current density in the PEFC stack.

3.3. Simple SOFC system and SOFC–PEFC systems

The configuration of the parallel and series SOFC–PEFC systems is shown in Fig. 4. The fuels for both cell stacks were assumed to be pure methane. The combustion exhaust gas from the SOFC stack is supplied to the heat exchanger and used to raise the air temperature. Gross dc output of the SOFC stack is converted to gross ac output by the inverter. Net ac output is determined by subtracting the power consumed in auxiliary machines from the gross ac output. The molar flow rate of methane for the SOFC M_{SO-CH_4} was determined so that the fuel utilization in the SOFC stack $U_{SO\text{-}FUEL}$ would be 85% when the J_{SO} is $2000\ A\,m^{-2}$ and the $W_{PE\text{-}Rated}$ is 0 kW (Note that the system is a simple SOFC system when the $W_{PE\text{-}Rated}$ is 0 kW). The $U_{SO\text{-}FUEL}$ is defined as

$$U_{SO-FUEL} \equiv \frac{I_{SO}}{8FM_{SO-CH_4}}, \quad (6)$$

where F is Faraday's constant. The reformed fuel is directly fed to the shift converter in the parallel SOFC–PEFC system, whereas the reformed fuel is fed to it via the tubular SOFC in the series SOFC–PEFC system. For the systems with PEFC stacks of various sizes, the flow rate of methane for the PEFC M_{PE-CH_4} was determined so that the fuel utilization of the PEFC stack $U_{PE\text{-}FUEL}$ would be 70%, which is the fuel utilization in an actual simple PEFC system [12], when both the J_{SO} and J_{PE} are

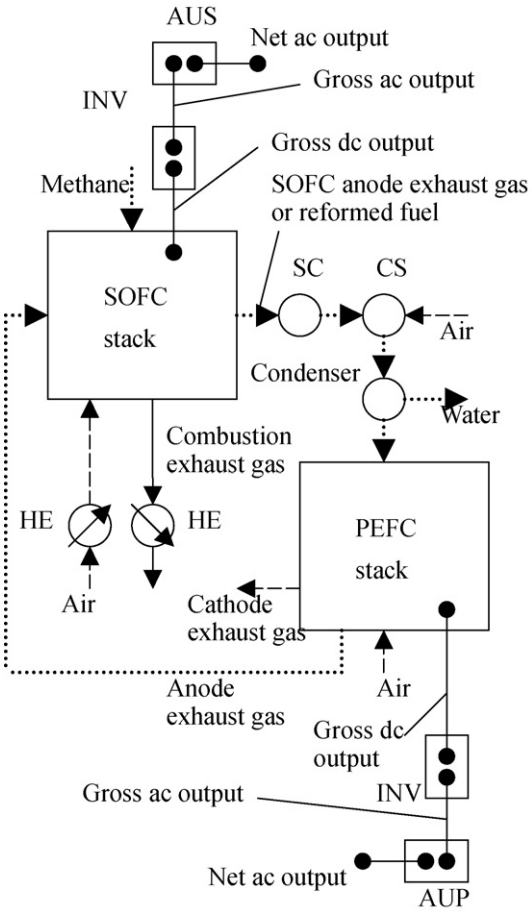

Fig. 4. Configuration of the SOFC–PEFC system. AUP, auxiliary machine for PEFC; AUS, auxiliary machine for SOFC; CS: CO selective oxidizer; HE, heat exchanger; INV, inverter; SC, Shift converter.

$2000\ A\,m^{-2}$ and the $U_{SO\text{-}FUEL}$ is 85%. The $U_{PE\text{-}FUEL}$ is assumed to be the ratio of the hydrogen used for power generation to that fed to the PEFC. That is, $U_{PE\text{-}FUEL}$ is defined as

$$U_{PE-FUEL} \equiv \frac{I_{PE}}{2FM_{PE-H_2}}, \quad (7)$$

where M_{PE-H_2} is the flow rate of hydrogen in the gas fed to the PEFC stack. The features of the parallel and series SOFC–PEFC systems are summarized in Table 1.

First, the performance of the systems with various sizes of PEFC stacks was calculated under the constant current density condition, in which the current densities in the both stacks were kept at $2000\ A\,m^{-2}$. And then, the current densities in the SOFC and PEFC stacks were varied so that total fuel utilization in the system $U_{SYS\text{-}FUEL}$ stayed constant in order to investigate the

Table 1
Features of SOFC–PEFC system

	Gas fed to the PEFC stack	Amount of reformed gas fed to the SOFC stack[a]	Amount of fuel fed to the PEFC stack[a]
Parallel SOFC–PEFC system	Reformed fuel	Constant	Increase
Series SOFC–PEFC system	SOFC anode exhaust gas	Increase	Increase

[a] Amount of gas for each stack as the rated output of PEFC stack increases.

effect of the proportion of fuel amount used in SOFC stack to that in PEFC stack. The $U_{\mathrm{SYS\text{-}FUEL}}$ is determined by

$$U_{\mathrm{SYS-FUEL}} = \frac{I_{\mathrm{SO}} + I_{\mathrm{PE}}}{8F(M_{\mathrm{SO-CH_4}} + M_{\mathrm{PE-CH_4}})}, \quad (8)$$

The total amount of fuel, $M_{\mathrm{SO-CH_4}} + M_{\mathrm{PE-CH_4}}$, stays constant when the current densities in the SOFC and PEFC stacks are varied.

The SOFC stack and the PEFC stack have an inverter and auxiliary machines. Like the net ac output of the SOFC stack, that of the PEFC stack was determined by subtracting the power consumed in auxiliary machines from the gross ac output, which is converted from gross dc output by using the inverter. The net ac output and electrical efficiency at net ac were calculated by the same equations as in our previous study [9,11].

4. Results and discussion

4.1. Parallel SOFC–PEFC system

The simulation results under the constant current density condition, in which the current densities of both stacks are kept at 2000 A m^{-2}, are discussed first. The relationship between the rated output of the PEFC stack $W_{\mathrm{PE\text{-}Rated}}$ and the heat used for steam reforming Q_{REF} and that between the $W_{\mathrm{PE\text{-}Rated}}$ and electrical efficiency at net ac η_{ac} are shown in Fig. 5. The simulation results at $W_{\mathrm{PE\text{-}Rated}}$ of 0 kW are those for the simple SOFC system. The Q_{REF} increases with $W_{\mathrm{PE\text{-}Rated}}$ since the heat used for the reforming of the PEFC fuel increases (see Fig. 3). The η_{ac} increases with $W_{\mathrm{PE\text{-}Rated}}$ because the Q_{REF} increases. Note that the SOFC exhaust heat contributes more effectively to the efficiency when the Q_{REF} increases. A PEFC stack with rated output of more than 80 kW cannot be operated in the parallel SOFC–PEFC system when the SOFC is 110 kW class. This is because the sufficient steam for the steam reforming reaction cannot be supplied by recycling the SOFC anode exhaust gas when the rated PEFC output exceeds a certain limit [9,11].

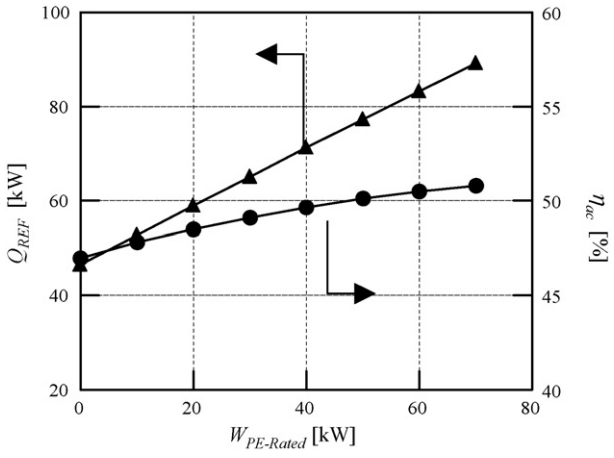

Fig. 5. The relationship between the rated output of the PEFC stack $W_{\mathrm{PE\text{-}Rated}}$ and the heat used for steam reforming Q_{REF} and that between $W_{\mathrm{PE\text{-}Rated}}$ and electrical efficiency at net ac η_{ac} in the parallel SOFC–PEFC system.

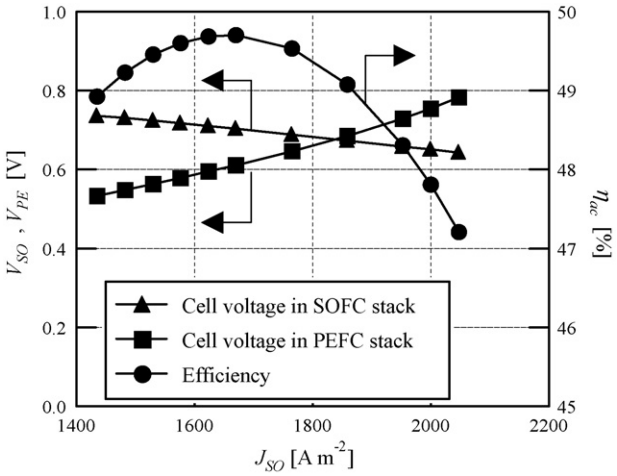

Fig. 6. The relationship between the current density in the SOFC stack J_{SO} and the cell voltages in both stacks V_{SO}, V_{PE} and that between the J_{SO} and the electrical efficiency at net ac η_{ac} in the parallel SOFC–PEFC system.

It is investigated how the η_{ac} is changed when the current densities of the both stacks are varied under the constant fuel utilization condition. The simulation result for the system with the PEFC stack with $W_{\mathrm{PE\text{-}Rated}}$ of 10 kW is shown in Fig. 6. Here, the amount of fuel was kept constant, though the current densities in both stacks were varied as mentioned in Section 3. The cell voltage in SOFC stack V_{SO} decreases with the current density in the SOFC stack J_{SO} since the ohmic voltage drop increases. On the contrary, the cell voltage in the PEFC stack V_{PE} increases with J_{SO}. This is because the current density in the PEFC stack J_{PE} decreases when J_{SO} increases in order to maintain the total fuel utilization in the system and because the decrement of J_{PE} causes the increment of V_{PE} (see Eq. (4)). There is an optimal J_{SO}, at which the η_{ac} is highest, since the V_{SO} decreases, but the $V_{\mathrm{PE\text{-}ac}}$ increases when J_{SO} decreases.

The relationships between J_{SO} and η_{ac} for the systems with the all size of PEFC stacks are summarized in Fig. 7. The system with the 20 kW-class PEFC stack has the optimal J_{SO} like the one with the 10 kW-class PEFC stack. On the contrary, η_{ac} monotonically increases when J_{SO} decreases in the systems with 30, 40, 50, 60 and 70 kW-class PEFC stacks. All systems would have the optimal J_{SO} if the J_{SO} could be decreased unlimitedly. However, J_{SO} cannot be decreased unlimitedly since sufficient steam for the steam reforming reaction cannot be supplied by recycling the SOFC anode exhaust gas when J_{SO} is less than some limit. Note that the amount of the recycling gas has to be increased when J_{SO} is decreased because the amount of steam that is included in the SOFC anode exhaust gas decreases when J_{SO} is decreased. The limit on J_{SO} is larger for the system with the larger PEFC stack. This is because a larger amount of steam has to be supplied when PEFC stack with a larger rated output is used.

The relationship between the $W_{\mathrm{PE\text{-}Rated}}$ and the maximum electrical efficiency in each system $\eta_{\mathrm{ac\text{-}Max}}$, which is derived from Fig. 7, is summarized in Fig. 8. The $\eta_{\mathrm{ac\text{-}Max}}$ is highest when $W_{\mathrm{PE\text{-}Rated}}$ is 40 kW. The $\eta_{\mathrm{ac\text{-}Max}}$ increases with $W_{\mathrm{PE\text{-}Rated}}$ when $W_{\mathrm{PE\text{-}Rated}}$ is smaller than 40 kW. The main reason for

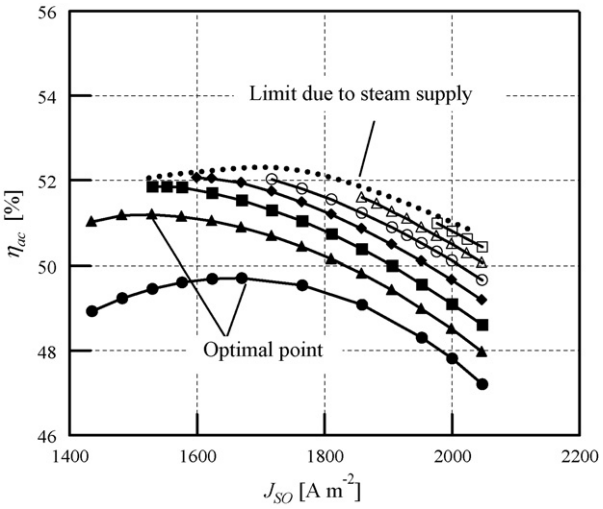

Fig. 7. The relationship between the current density in the SOFC stack J_{SO} and the electrical efficiency at net ac η_{ac} in the parallel SOFC–PEFC system. (●) System with 10-kW-class PEFC stack; (▲) system with 20-kW-class PEFC stack; (■) system with 30-kW-class PEFC stack; (♦) system with 40-kW-class PEFC stack; (◯) system with 50-kW-class PEFC stack; (△) system with 60-kW-class PEFC stack; (□) system with 70-kW-class PEFC stack.

this is that Q_{REF} increases with $W_{PE\text{-}Rated}$, i.e., SOFC exhaust heat contributes to $\eta_{ac\text{-}Max}$ via Q_{REF}. The $\eta_{ac\text{-}Max}$ decreases with $W_{PE\text{-}Rated}$ when the $W_{PE\text{-}Rated}$ is larger than 40 kW. This is because J_{SO} cannot be decreased enough due to the limit on the steam supply when $W_{PE\text{-}Rated}$ is larger than 40 kW. It is very interesting that the highest $\eta_{ac\text{-}Max}$ in the all systems is achieved in the system with a 40 kW-class PEFC stack. When the average current densities of both stacks are kept constant, the system with a larger PEFC stack always has higher η_{ac} than the one with a smaller PEFC stack. However, there is an optimal size of the PEFC stack at which the $\eta_{ac\text{-}Max}$ is highest for the parallel SOFC–PEFC system when the average current density is adjusted under the constant fuel utilization condition.

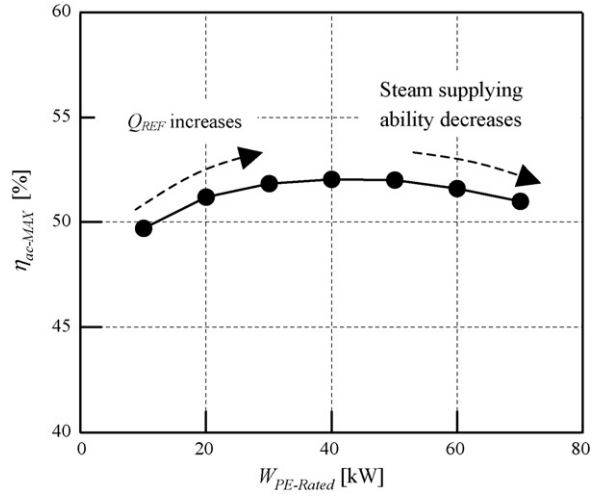

Fig. 8. The relationship between the rated output of the PEFC stack $W_{PE\text{-}Rated}$ and the maximum electrical efficiency in each system $\eta_{ac\text{-}Max}$ in the parallel SOFC–PEFC system.

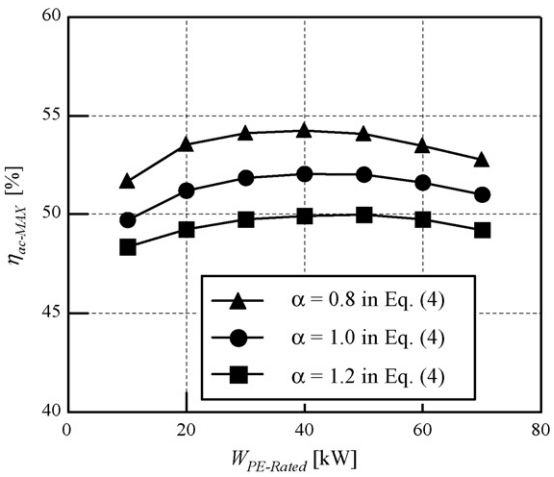

Fig. 9. The relationship between the rated output of the PEFC stack $W_{PE\text{-}Rated}$ and the maximum electrical efficiency in each system $\eta_{ac\text{-}Max}$ in the parallel SOFC–PEFC system.

Next, it is investigated how the relationship between $W_{PE\text{-}Rated}$ and $\eta_{ac\text{-}Max}$ changes when the IV characteristics of the PEFC stack are varied. The relationship between $W_{PE\text{-}Rated}$ and $\eta_{ac\text{-}Max}$ when the value of α is 0.8, 1.0 or 1.2 in Eq. (4) is shown in Fig. 9. The $\eta_{ac\text{-}Max}$ is higher when the IV characteristics of the PEFC stack are better (when α is smaller). It is very interesting that the systems with a 40 kW-class PEFC stack has the highest $\eta_{ac\text{-}Max}$ despite the variation of the IV characteristics in this range.

4.2. Series SOFC–PEFC system

The relationship between $W_{PE\text{-}Rated}$ and Q_{REF} and that between $W_{PE\text{-}Rated}$ and η_{ac} under the constant current density condition are shown in Fig. 10. The current densities of the both stacks are kept at 2000 A m^{-2}. The Q_{REF} and η_{ac} increase with $W_{PE\text{-}Rated}$ like in the parallel SOFC–PEFC system. The increasing ratio of η_{ac} to the increment of $W_{PE\text{-}Rated}$ is higher in the series SOFC–PEFC system than in the parallel SOFC–PEFC

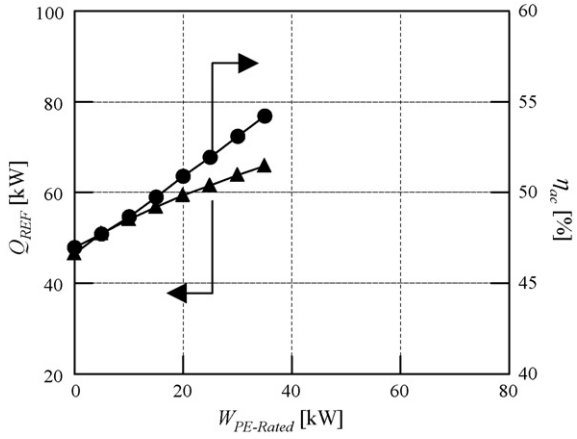

Fig. 10. The relationship between the rated output of the PEFC stack $W_{PE\text{-}Rated}$ and the heat used for steam reforming Q_{REF} and that between $W_{PE\text{-}Rated}$ and electrical efficiency at net ac η_{ac} in the series SOFC–PEFC system.

system. This is because V_{SO} increases with $W_{PE\text{-}Rated}$ in the series SOFC–PEFC system, but is almost constant in the parallel SOFC–PEFC system: The amount of reformed gas fed to the SOFC stack increases with $W_{PE\text{-}Rated}$ in the series SOFC–PEFC system but it stays constant in the parallel SOFC–PEFC system.

A PEFC stack with rated output of larger than 40 kW cannot be operated in the series SOFC–PEFC system when the SOFC is 110 kW class. The limit is lower for the series SOFC–PEFC system than for the parallel SOFC–PEFC system. This is because the molar fraction of steam in the SOFC anode exhaust gas is lower in the series SOFC–PEFC system, since a larger amount of reformed fuel is fed to the SOFC stack in the series SOFC–PEFC system. Much more SOFC exhaust gas has to be recycled to feed sufficient steam for the same amount of fuel for the PEFC in the series SOFC–PEFC system. Therefore, the maximum rated output of a PEFC stack that can be operated in the series SOFC–PEFC system is lower.

The relationship between J_{SO} and η_{ac} under the constant fuel utilization condition is shown in Fig. 11. The system with a 5 kW-class PEFC stack has the optimal J_{SO}, at which η_{ac} is highest. The systems with a 10, 15, 20, 25, 30 and 35 kW-class PEFC stacks do not have the optimal J_{SO} because it is limited due to water. Here, there are significant differences between the parallel and series SOFC–PEFC systems. Though there is an optimal size of the PEFC stack at which the $\eta_{ac\text{-}Max}$ is highest in the parallel SOFC–PEFC system, the system with a larger PEFC stack always has higher $\eta_{ac\text{-}Max}$ than the one with a smaller PEFC stack in the series SOFC–PEFC system as shown in Fig. 12. The reason for this is as follows. In the parallel SOFC–PEFC system, the increment of the rated output of the PEFC stack causes the increment of the SOFC exhaust heat used for the steam reforming, which is the main contribution to the electrical efficiency in the system. On the contrary, in the series SOFC–PEFC system, the increment of the PEFC stack causes the increment of the

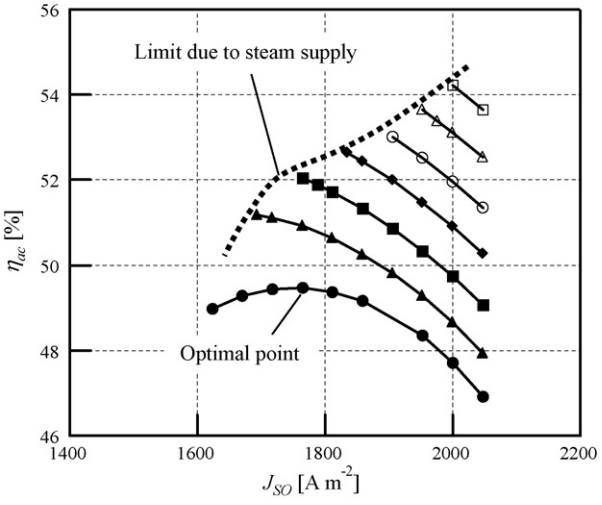

Fig. 11. The relationship between the current density in the SOFC stack J_{SO} and the electrical efficiency at net ac η_{ac} in the series SOFC–PEFC system. (●) System with 5 kW-class PEFC stack; (▲) system with 10 kW-class PEFC stack; (■) system with 15 kW-class PEFC stack; (♦) system with 20 kW-class PEFC stack; (◯) system with 25 kW-class PEFC stack; (△) system with 30 kW-class PEFC stack; (□) system with 35 kW-class PEFC stack.

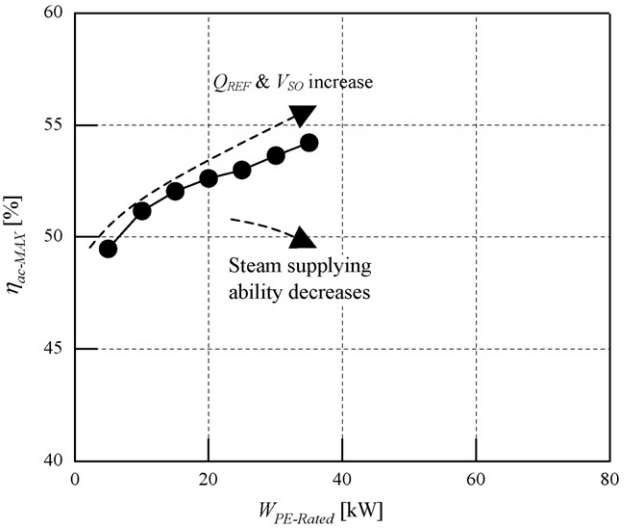

Fig. 12. The relationship between the rated output of the PEFC stack $W_{PE\text{-}Rated}$ and the maximum electrical efficiency in each system $\eta_{ac\text{-}Max}$ in the series SOFC–PEFC system.

SOFC exhaust heat used for the steam reforming and the increment of the cell voltage in the SOFC stack, both of which are the main positive contributions to the electrical efficiency in the system. Therefore, the increment of the PEFC stack output has a larger effect on η_{ac} in the series SOFC–PEFC system than in the parallel SOFC–PEFC system. As a result, the increment of $W_{PE\text{-}Rated}$ always leads to the increment of $\eta_{ac\text{-}Max}$ in the series SOFC–PEFC system, though the increment of η_{ac} caused by the current density adjustment becomes smaller with $W_{PE\text{-}Rated}$ since the steam-supplying ability decreases. Note that the increasing ratio of $\eta_{ac\text{-}Max}$ to the increment of $W_{PE\text{-}Rated}$ is lower when the $W_{PE\text{-}Rated}$ is larger, because of the lower steam-supplying ability.

The relationship between $W_{PE\text{-}Rated}$ and $\eta_{ac\text{-}Max}$ when the value of α is 0.8, 1.0 or 1.2 in Eq. (4) is shown in Fig. 13. It is very interesting that the system with a larger PEFC stack always has

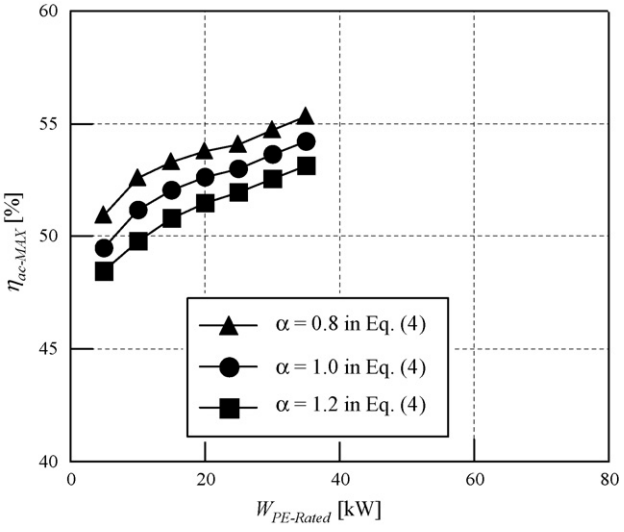

Fig. 13. The relationship between the rated output of the PEFC stack $W_{PE\text{-}Rated}$ and the maximum electrical efficiency in each system $\eta_{ac\text{-}Max}$ in the series SOFC–PEFC system.

higher $\eta_{\text{ac-Max}}$ than the system with smaller one even though the IV characteristic of the PEFC stack is varied in the series SOFC–PEFC system. This tendency is quite different from that in the parallel SOFC–PEFC system as mentioned above.

5. Conclusions

The effect of the current densities in the SOFC and PEFC stacks on the performance of a SOFC–PEFC combined system was evaluated under a constant fuel utilization condition by numerical simulation. It was found that the SOFC–PEFC system has an optimal combination of current densities, for which the electrical efficiency is highest, because the cell voltage in one stack increases while that of the other stack decreases when the current densities are changed under the constant fuel utilization condition. It was demonstrated that there is an optimal size of the PEFC stack in the parallel SOFC–PEFC system from the viewpoint of efficiency, although a larger PEFC stack always leads to higher electrical efficiency in the series SOFC–PEFC system. This tendency does not change, though the voltage drop ratio in the PEFC stack to the current density is varied by +20 or −20%.

References

[1] J. Larminie, A. Dicks, Fuel Cell Systems Explained, second ed., John Wiley and Sons, 2003, pp. 163–176.
[2] R.A. George, J. Power Sources 86 (2000) 134–139.
[3] J. Larminie, A. Dicks, Fuel Cell Systems Explained, second ed., John Wiley and Sons, 2003, pp. 213–224.
[4] S.E. Veyo, W.L. Lundberg, Proceeding of the International Gas Turbine and Aeroengine Congress and Exhibition, 1999 (paper 1999-GT-550).
[5] S.E. Veyo, L.A. Shockling, J.T. Dedere, J.E. Gillett, W.L. Lundberg, Proceeding of the International Gas Turbine and Aeroengine Congress and Exhibition, 2000 (paper 2000-GT-550).
[6] T.W. Song, J.L. Sohn, J.H. Kim, T.S. Kim, S.T. Ro, K. Suzuki, J. Power Sources 142 (2005) 30–42.
[7] H.E. Vollmar, C.U. Maier, C. Nolscher, T. Merklein, M. Poppinger, J. Power Sources 86 (2000) 90–97.
[8] A.L. Dicks, R.G. Fellows, C.M. Mescal, C. Seymour, J. Power Sources 86 (2000) 501–506.
[9] M. Yokoo, T. Take, J. Power Sources 137 (2004) 206–215.
[10] M. Yokoo, K. Watanabe, M. Arakawa, Y. Yamazaki, J. Power Sources 153 (2006) 18–28.
[11] M. Yokoo, K. Watanabe, M. Arakawa, Y. Yamazaki, J. Power Sources 159 (2006) 836–845.
[12] T. Yateke, A. Sonai, S. Matsuda, A. Kano, Proceedings of Fuel Cell Symposium, 2001, pp. 76–83 (in Japanese).